Dynamic Response of Concrete-Faced Rockfill Dams to Strong Seismic Excitation

By Nasim Uddin,[1] and George Gazetas,[2] Members, ASCE

Abstract: A dynamic plane-strain finite-element study of the response of a typical 100-m-tall concrete-faced rockfill (CFR) dam to strong seismic shaking is presented. The rockfill is modeled as an equivalent-linear material, whose strain-dependent shear modulus is proportional to the square root of the confining pressure. Coulomb's friction law governs the behavior of the interface between face slab and dam, and slippage is allowed to occur whenever the seismic shear tractions exceed the pertinent frictional capacity. Two sets of historic accelerograms, with peak ground accelerations (PGA) of about $0.40g$ and $0.60g$, respectively, are used as excitation. Numerical results highlight key aspects of the seismic response of CFR dams with emphasis on the internal forces developing in the slab. It is shown that slab distress may be produced only from axial tensile forces, developing due mainly to the rocking component of dam deformation. For the $0.60g$ shaking tensile stresses that are much higher than the likely tensile strength of concrete develop in the slab. The presented results do not account for potentially detrimental three-dimensional (3D) narrow-canyon effects.

INTRODUCTION: CONCRETE-FACED ROCKFILL (CFR) DAM

The basic features of the CFR dam are outlined here with the help of Fig. 1, which shows a cross section and some characteristic details of a typical design. In contrast with the earth-core rockfill (ECR) dam, the main body of the CFR dam consists exclusively of rockfill, all of which is located downstream from the water thrust. The latter acts externally on the upstream reinforced-concrete face and contributes to increasing the stiffness and stability of CFR dams. Therefore, much steeper slopes (ranging from 1V:1.3H to 1V:1.6H) are attainable in CFR dams.

The face slab is usually made of 20-MPa-strength concrete, with 0.4% reinforcing in each direction, placed in the middle of the slab. The slab thickness varies along the height, starting at 0.30–0.40 m near the crest and increasing by approximately 0.002 h_w, where h_w = depth of water (in meters). Crucial to safety is the design and construction of the perimetric joint between face slab and the so called plinth, a concrete block anchored into the ground [Fig. 1(d)], as this joint always opens up and distorts moderately when the reservoir is filled. A double and sometimes triple line of defence is provided against this potential source of leakage [see items 1, 2, 4, 5, and 6 in Fig. 1(e)].

Face slabs are placed in vertical strips, typically 15 m wide, by slip form continuously from bottom to top, where they culminate in an L-shaped 3-m- to 5-m-high cantilever crest wall. The cost of the slab is more than offset by saving a slice of downstream rockfill (Fitzpatrick et al. 1985). The upstream zone supporting the face slab consists of smaller-size rock than the main body of the dam in order to facilitate slope trimming and compaction, and thus minimize differential slab movements. Another role of this relatively low permeability zone is to limit leakage into the dam to that which could safely be passed through the downstream zones, should the cofferdam be overtopped before the concrete-face slab is constructed.

Compaction of the rockfill to a high density is required to minimize deformations and face-slab distress and leakage. One of the factors controlling the stiffness of rockfill is its gradation. Well-graded materials, with smaller-size particles filling the voids between larger rocks yet maintaining free-draining characteristics, have led to very satisfactory design. High-deformation moduli have in fact been achieved in CFR dams with rockfill having uniformity coefficient of 20 or higher and containing about 30% of material smaller than 25 mm (1 in.). Measurements have also shown that rockfill is about three times stiffer in the horizontal than in the vertical direction [see Cook and Sherard (1985), and Fitzpatrick et al. (1985) for details].

SEISMIC BEHAVIOR: LITERATURE REVIEW

The concrete-faced rockfill (CFR) dam has been used in many parts of the world with increasing frequency in recent years. In addition to being a natural choice where suitable clayey core material is not available in the vicinity of the project, the CFR dam has in many cases

[1]Engr., Acres International, Amherst, NY 14228-1180.
[2]Prof. of Civ. Engrg., State Univ. of New York, Buffalo, NY 14260.

Note. Discussion open until July 1, 1995. To extend the closing date one month, a written request must be filed with the ASCE Manager of Journals. The manuscript for this paper was submitted for review and possible publication on August 12, 1993. This paper is part of the *Journal of Geotechnical Engineering*, Vol. 121, No. 2, February, 1995. ©ASCE, ISSN 0733-9410/95/0002-0185–0197/$2.00 + $.25 per page. Paper No. 6778.

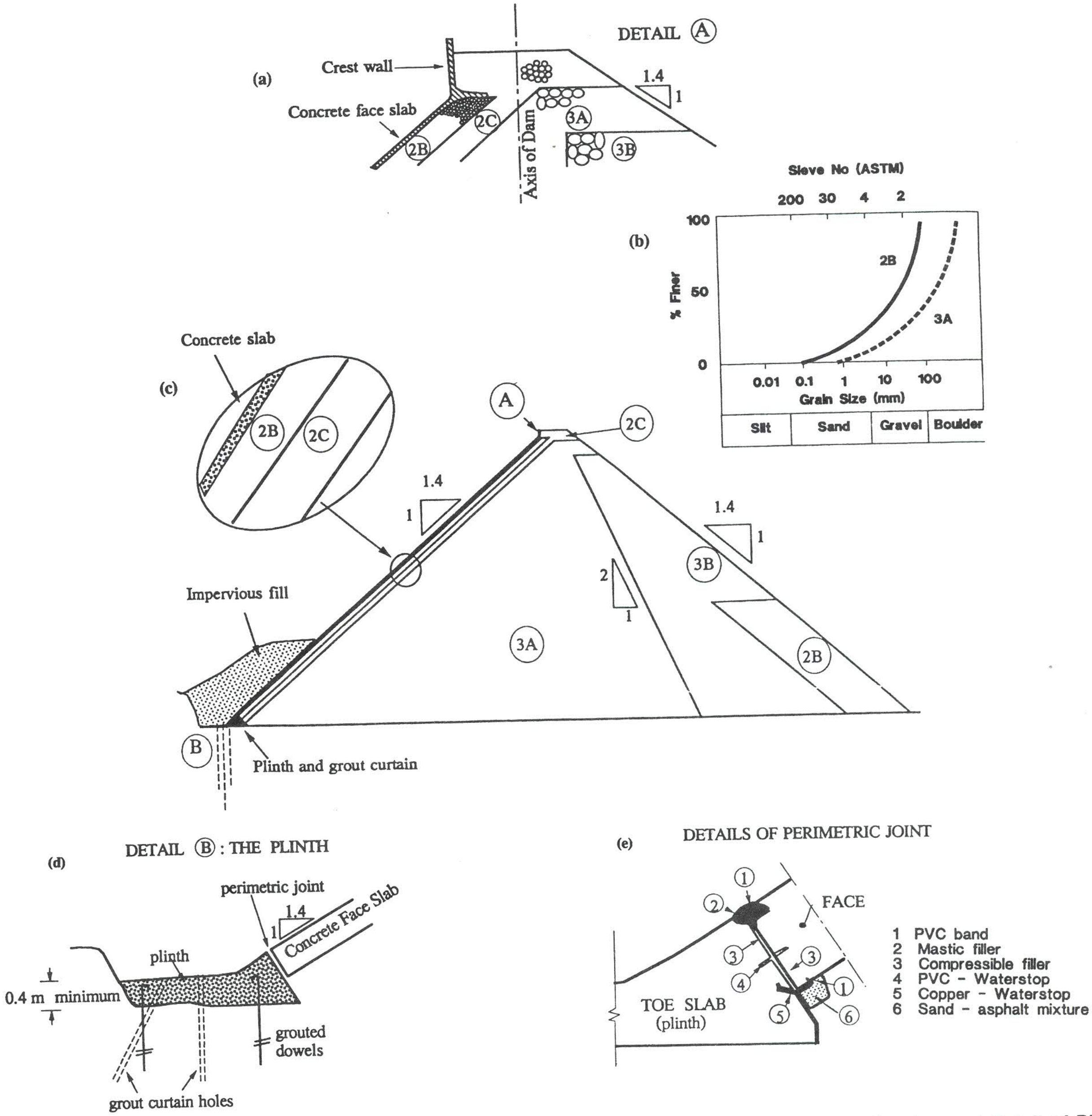

FIG. 1. CFR Dam: (a) Detail of Crest; (b) Material Composition; (c) Typical Cross Section; (d) Cross Section and Detail of Plinth; (e) Cross Section and Detail of Parametric Joint

been found to be the least-cost alternative. As worldwide experience with the long-term performance of CFR dams is growing, their popularity may well increase in the coming years. Current design trends and construction/performance records of many recent dams can be found in the proceedings of a 1985 ASCE symposium (Cooke and Sherard 1985) and an accompanying issue of the ASCE *Journal of Geotechnical Engineering* (Sherard and Cooke 1987).

The anticipated seismic response and performance of modern CFR dams has received only limited attention in published literature (Guros et al. 1984; Seed et al. 1985; Arrau et al. 1985; Bureau et al. 1985; Han et al. 1988; Gazetas and Dakoulas 1992). Many engineers have argued that the CFR dam is inherently safe against potential seismic damage (Sherard and Cooke 1987) since: (1) The entire CFR embankment is dry and hence earthquake shaking cannot cause pore-water pressure buildup and strength degradation; and (2) the reservoir water pressure acts externally on the upstream face and hence the entire rockfill mass acts to provide stability, whereas by contrast in earth-core rockfill (ECR) dams this may be true only for the downstream rockfill shell. Notwithstanding the merit of these arguments, it is pointed out that, to date, no modern CFR dam has been tested under strong seismic shaking to prove or disprove the adequacy of its various design features. In fact, most CFR dams have been built in areas of extremely low seismicity, such as Australia and Brazil, and it seems that some of the design concepts and features have evolved with no consideration to their seismic performance.

Seed et al. (1985) reported a set of conventional finite-element (FE) analyses aimed at estimating the magnitude of sliding deformations of typical CFR dams subjected to base accelerations with a peak of $0.50g$, originating at sources of magnitude ranging from 6.5 to 8.25. Conventional FE means an analysis in which the discretization does not include the face slab, which is thus not taken into account. Their analyses were performed in two stages, accepting the well-established decoupling of the "elastic" dynamic response analysis from the inelastic sliding deformation analysis. In the first stage, equivalent-linear plane-strain analyses were conducted, appropriate for tall dams built in very wide valleys. In the second stage, permanent deformations were computed using the Makdisi and Seed (1979) version of the 1965 Newmark "sliding-block" concept. For an angle of shearing resistance at low confining pressures equal to 54°, Seed et al. (1985) found that the computed deformations for the downstream slope are less than 0.30 m, for a magnitude of 7.5 or less. However, with magnitude of about 8.25, deformations as large as 2 m may occur (due to the larger number of cycles of motion) in the downstream direction. Such deformations are undesirably high, and would require flatter slopes to limit the movements to acceptable values. Finally, Seed et al. (1985) made recommendations for the required slopes, so that the sliding deformations would not exceed 0.50 m. The recommended values are appreciably flatter than the slopes currently used in design; in areas of high and very high seismicity they are of the order of 1.6H:1V or flatter.

Bureau et al. (1985) presented a study dealing with the seismic performance of rockfill dams in general, and the possible modes of failure of CFR dams in particular. A numerical formulation was outlined for computing the nonlinear response of CFR dams and evaluating the complete distribution pattern of permanent deformations without the need to use the simplified Newmark procedure. In addition, an equivalent-linear finite-element formulation was utilized to study the effect of fluid-dam interaction and to estimate the seismic axial forces and bending moments on the concrete-face slab. Among their conclusions were the following: (1) Hydrodynamic effects can be safely ignored in the seismic response of CFR dams; (2) most of the dam section under strong base excitation (PGA = $0.70g$) is in a state of plastic deformation, thus "distributed slumping," rather than failure along a discrete surface, may take place; (3) permanent deformations seem to concentrate in the upper third of the dam, a result confirmed by observations on El Infiernillo Dam in Mexico [e.g., Elgamal et al. (1990)]; and (4) deformation of the order of 1 m remains in the crest following a strong shaking. They concluded that crest settlements of modern CFR dams would not exceed 1–2% of the dam height under severe earthquake shaking.

A crude qualitative picture of the mechanism of seismic failure of CFR dams might be obtained through shaking-table tests on small-scale physical models. Such a study, reported by Han et al. (1988), used a 1-m-high model with both slopes equal to 1.4H:1V, a 4-mm-thick face slab consisting mainly of gypsum and having a tensile strength of up to 300 kPa, a 2.5-cm-thick supporting zone of sand with mass density of 1.7 Mg/m^3, and a main body consisting of sand and gravel compacted to a 1.6 Mg/m^3 density. Base acceleration reached $0.60g$, but permanent deformations started at $0.14g$. It was observed that initial sliding was confined to shallow wedges in the vicinity of the crest. With increasing acceleration amplitudes, the size of sliding zone increased. At even greater amplitudes the face slab lost support, deformed as a cantilever, and ruptured in violent vibration. These observations support the concept of sliding mode of deformation predicted in the theoretical studies. However, in view of the inadequacy of such small-scale models to reproduce the significant effects of gravity on material behavior, the results of this study should be viewed with great caution, and only qualitatively. It would be of interest to attempt realistic modeling of CFR dams in a large centrifuge; the writers are not aware of any such study up to now.

Gazetas and Dakoulas (1992) have studied the 3D seismic response of an actual 120-m-tall CFR dam that is presently under construction in a narrow canyon (of approximately semicylindrical shape), and concluded that tall CFR dams in such narrow canyons of solid rock may experience extremely intense shaking at midcrest during strong seismic events — a direct consequence of wave "focusing" effects, enhanced by the very stiff and "unyielding" rockfill of the CFR dam. Still the overall integrity of the dam may not be in much danger. However, some rather significant deformation problems are likely to occur: nonuniform permanent distortions, cracking of and leakage through the concrete slab, settlement of the crest that would reduce the available freeboard, and failure of the crest retaining wall ("parapet"). With respect to the latter, they suggested an improved soil support and a substantial decrease in the wall height (from the originally planned 6 m).

An important missing point in all of these studies is that no study has been made of the internal forces/stresses developing in the face slab. The potential consequences of strong seismic shaking for CFR dams is explored here with the help of state-of-the-art FE analyses of a typical 100-m-tall dam. Attempting to fill the apparent gap, particular emphasis is accorded to the internal forces developing in the face slab during earthquake.

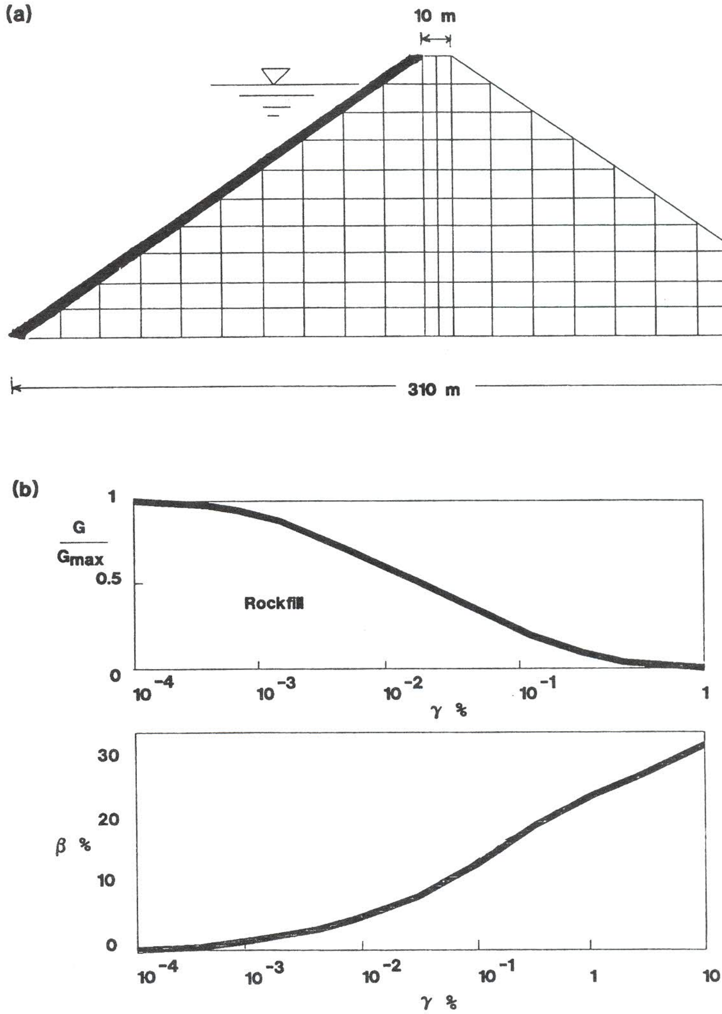

FIG. 2. Studied Typical CFR Dam: (a) Dam Geometry; (b) Shear Modulus and Damping Ratio versus Cyclic Shear Strain of Rockfill

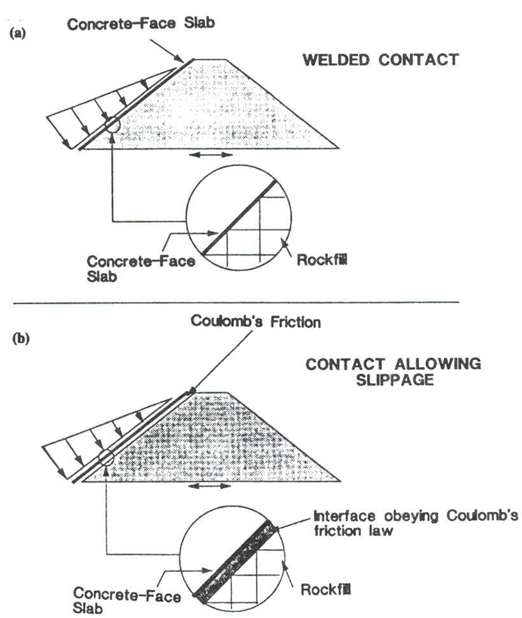

FIG. 3. Schematic Representation of Contact: (a) Welded; (b) Frictional (Allowing Slippage)

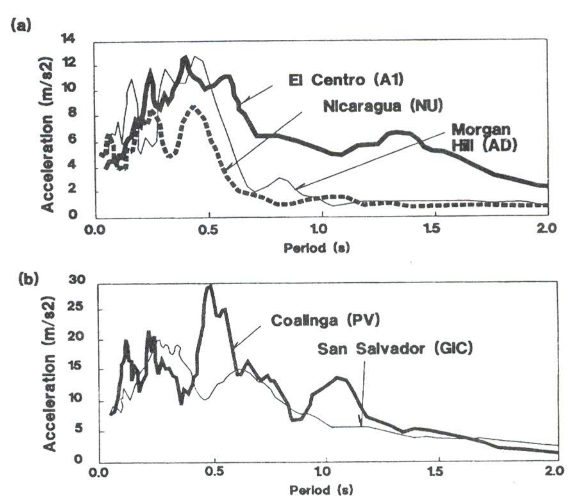

FIG. 4. Response Spectra: (a) Moderately Strong Earthquake Records; (b) Very Strong Earthquake Records

TABLE 1. Characteristics of Historic Records Used in Time-History Analysis

Earthquake name (1)	Style of rupture mechanism (2)	M_s (3)	Record (station) name (4)	Distance to source (km) (5)	Site geology (6)	PGA (g) (7)
San Salvador (October 1986)	strike-slip	5.4	Geotechnical Investigation Center (GIC)	4	bedrock	0.69
Coalinga (May 1983)	reverse	6.5	Pleasent Valley (PV)	11	Franciscan formation	0.60
Imperial Valley (October 1979)	strike-slip	6.9	El Centro Station No. 1 (A1)	8	alluvium	0.37
Nicaragua (March 1973)	strike-slip	6.2	National University (NU)	6	sediment	0.36
Morgan Hill (April 1984)	strike-slip	6.1	Anderson Dam Abutment (AD)	4	bedrock	0.42

TABLE 2. Calculated Natural Frequencies of 100-m-Tall CFR Dam

Mode (1)	Without slab (Hz) (2)	With slab (Hz) (3)
1	1.029	1.056
2	1.590	1.596
3	1.850	1.893
4	2.255	2.285
5	2.535	2.571
6	2.683	2.720
7	3.050	3.136
8	3.102	3.185
9	3.529	3.562
10	3.676	3.721

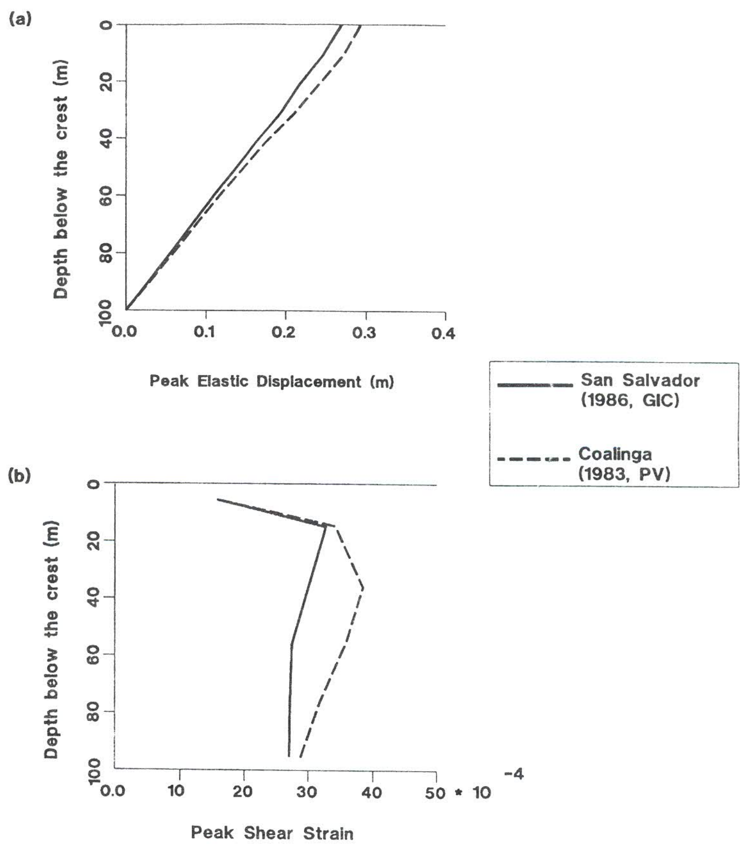

FIG. 5. Distribution along Vertical z-Axis: (a) Peak Relative "Elastic" Displacement; (b) Peak Shear Strain in Rockfill for Very Strong Excitation (PGA > 0.60g)

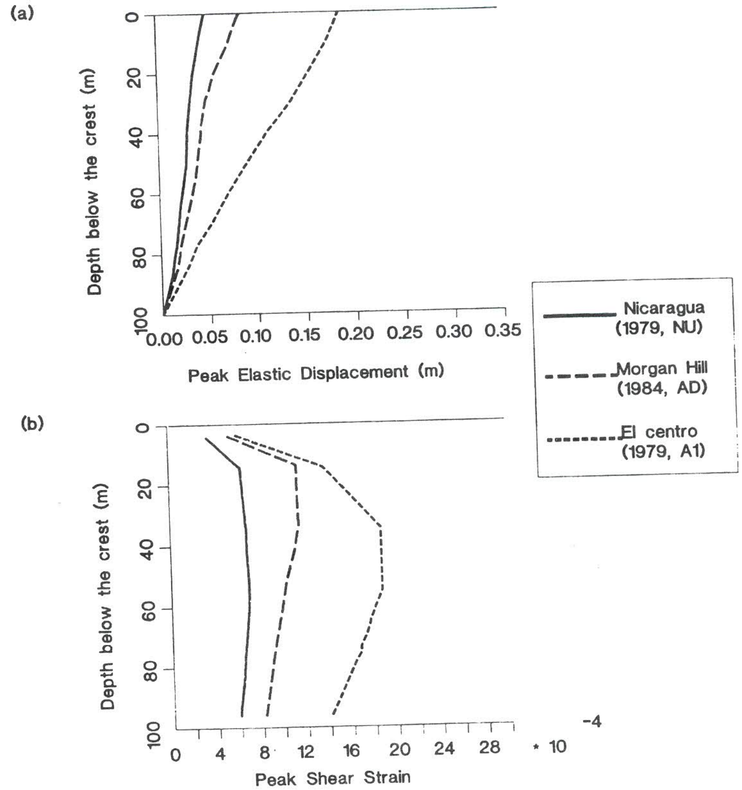

FIG. 6. Distribution along Vertical z-Axis: (a) Peak Relative Elastic Displacement; (b) Peak Shear Strain in Rockfill for Moderately Strong Excitation (PGA $\simeq$ 0.40g)

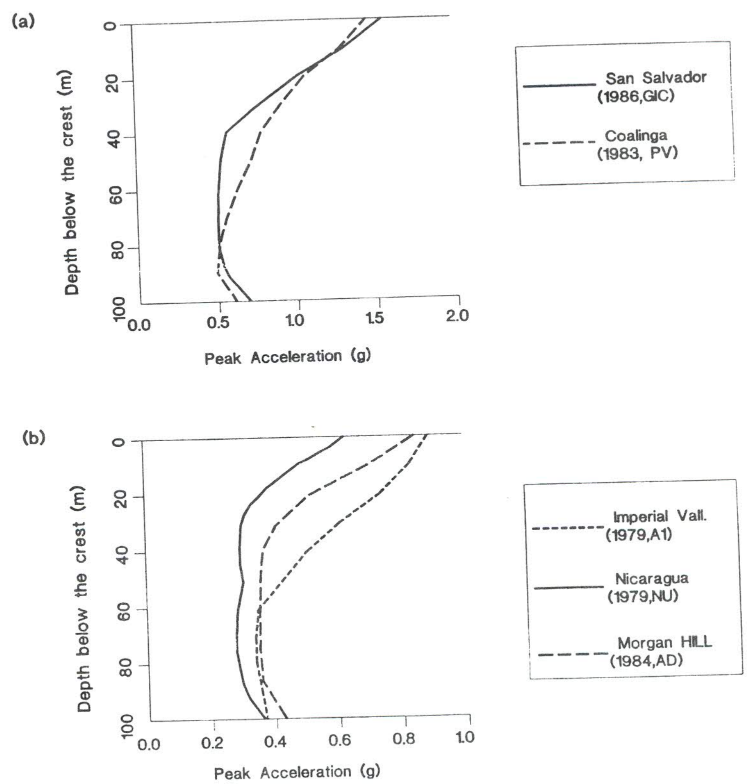

FIG. 7. Distribution along Vertical z-Axis of Peak Absolute Acceleration: (a) Very Strong Excitation (PGA > 0.60g); (b) Moderately Strong Excitation (PGA $\simeq$ 0.40g)

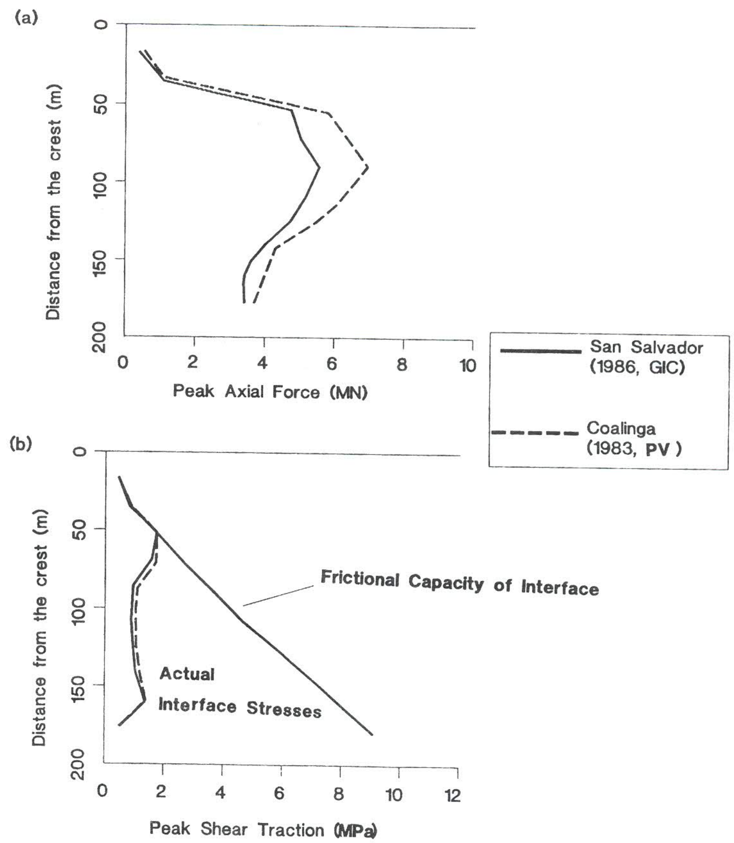

FIG. 8. Distribution along Slab: (a) Peak Axial Force; (b) Peak Shear Traction along Slab-Rockfill Interface for Very Strong Shaking (PGA > 0.60g) with Frictional Contact (Allowing both Slippage and Separation)

GEOMETRY AND MATERIALS OF STUDIED DAM

The typical 100-m-tall dam studied here is symmetric with two 1.5H:1V slopes and with a 0.40-m-thick concrete-face slab. The crest is 10 m wide and the reservoir is at its maximum level, 90 m above the base.

The dynamic behavior of a rockfill element is described through: (1) The small-strain shear modulus, G_{max}; (2) the decrease of secant modulus G with increasing strain γ; (3) the hysteretic damping ratio, β, which is an increasing function of the amplitude of shear strain γ; and (4) the Poisson's ratio, ν. Published experimental results from the literature were utilized to assign realistic values to the material parameters (Seed et al. 1986). Thus, the spatial distribution of G_{max} was estimated as a function of the effective confining pressure, $\sigma_m = (\sigma_1 + \sigma_2 + \sigma_3)/3$, of each rockfill element

$$G_{max} = 1{,}000(K_2)_{max}(\sigma_m)^{1/2} \tag{1}$$

Here, $(K_2)_{max}$ has units of square root of stress, and its value for compacted gravels and rockfill is in the range of 40–70 if stresses are in kPa (or about 150–250 if stresses are in lb/sq ft). Back analysis by Mejia et al. (1982) of the response of the Orovile Dam in California to a weak seismic shaking gave $(K_2)_{max} = 170$ (stress units in lb/sq ft). In view of the greater compaction likely to be achieved by modern equipment, $(K_2)_{max} = 200$ is used as a typical best estimate in our dynamic response analyses. $(K_2)_{max}$ is also varied parametrically between 150 and 250, if only to confirm that the conclusions regarding the performance of the dam are not sensitive to the exact value of this parameter. Static analyses are first carried out using the FE code ADINA (Bathe et al. 1988) to obtain the effective mean principal stress σ_m in all elements.

Poisson's ratio ν for dry or nearly dry rockfill is taken equal to 0.25. Note that while ν has only a marginal influence on lateral oscillations, it may play an appreciable role in rocking, longitudinal, and especially vertical oscillations (Gazetas 1981a, b).

Some limited data are available for estimating the decline of secant shear modulus, G, with increasing γ, in rockfill; they reveal a slightly faster rate of decline than for sandy soils [e.g., Seed et al. (1986)]. On the other hand, the data for the dependence of β on γ show a slightly faster rate of increase than for sands and clays.

Having modeled the plane geometry and dynamic properties of the dam, iterative 2D equivalent-linear viscoelastic analyses were performed in which the shear modulus, G, and damping

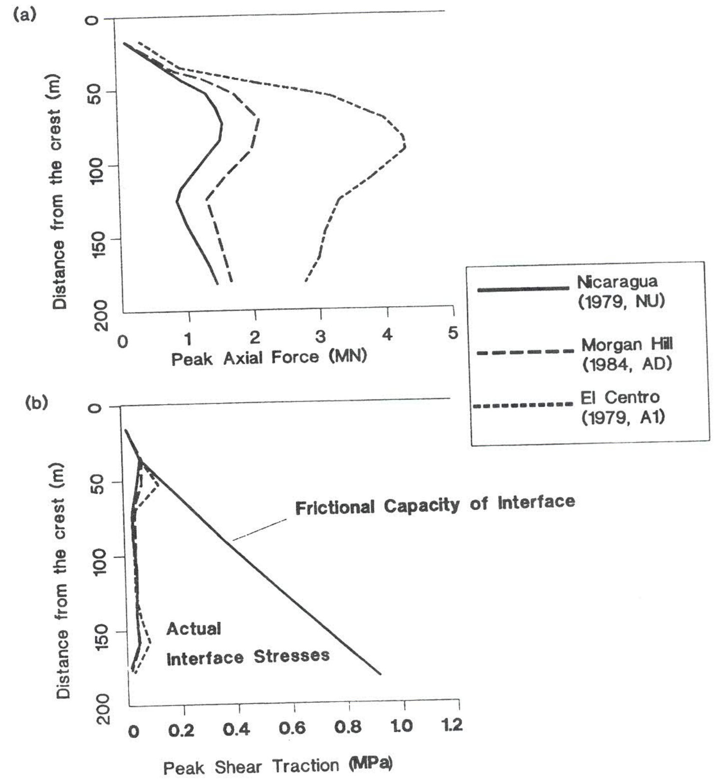

FIG. 9. Distribution along Slab: (a) Peak Axial Force; (b) Peak Shear Traction along Slab-Rockfill Interface for Moderately Strong Shaking (PGA ≃ 0.4*g*) with Frictional Contact (Allowing both Slippage and Separation)

ratio, β, were obtained from the effective shear strain level of the previous iteration. The effective shear strain was assumed to be 2/3 of the peak shear strain. All analyses were performed using ADINA, which incorporates Newmark's time-integration algorithm for a direct step-by-step solution.

NUMERICAL MODEL AND GROUND MOTION

The dam section is discretized in 150 finite elements as shown in Fig. 2(a). The concrete face is in a simple tensionless contact with the upstream body of the rockfill dam. This contact obeys Coulomb's friction law, with the hydrostatic load providing the normal forces to resist sliding. Fig. 3(a and b) shows both "welded" and "frictional" contact between the concrete-face slab and rockfill.

The face slab is discretized into a set of plane-strain beam elements. To model the slip and separation at the interface during the strong earthquake shaking, special joint elements in ADINA are utilized. These elements can reproduce realistically in the time-domain slippage and reattachment between slab and the supporting soil, as well as separation (uplifting) of the slab from the soil whenever net tensile stresses are about to develop. The procedure used by ADINA is an iterative one. Any segment of the slab experiences sliding if the ratio of the computed tangential to the normal forces is about to exceed the coefficient of friction. The tangential force is then updated to equal the local frictional capacity, which is essentially equal to the water pressure multiplied by coefficient of friction. Implementation of this assumption requires a fine enough FE discretization and relatively small load steps during the solution. A comprehensive sensitivity study has been reported by Uddin (1992) that confirmed the adequacy of the utilized discretization. Further verification studies of the models included computation of the natural frequencies of the dam and comparison with published solutions (Uddin 1992; Gazetas and Uddin 1994).

In this study, accelerograms recorded in five historic earthquakes are used as the input ground motion. Information on the records and the earthquake events are summarized in Table 1. Based on the peak ground acceleration (PGA) and distance from the source, these five records are divided into two groups:

- Very strong motion (PGA ≥ 0.6*g*): Geotechnical Investigation Center (GIC) record in the San Salvador (October 1986) earthquake, and Pleasent Valley (PV) record in the Coalinga (May 1983) earthquake.

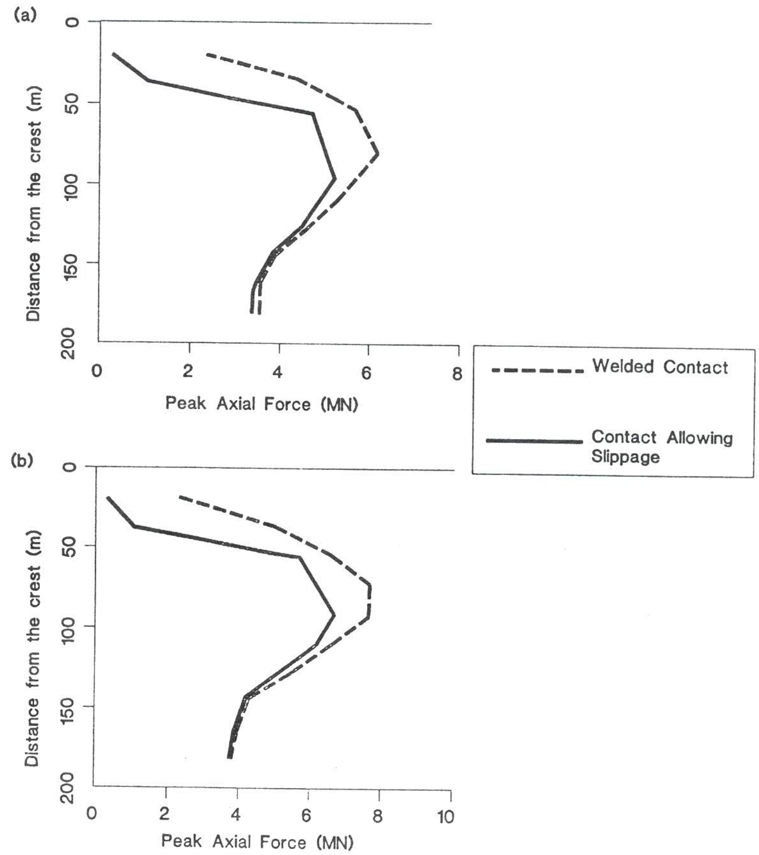

FIG. 10. Effect of Type of Slab-Dam Interface Behavior on Distribution of Peak Axial Force in Slab: (a) 1986 San Salvador GIC Excitation; (b) 1983 Coalinga PV Excitation

- Moderately strong motion (PGA $\approx 0.4g$): El Centro A1 station in the Imperial Valley (October 1979) earthquake, National University (NU) record in the Nicaragua (March 1973) earthquake, and Anderson Dam Abutment (AD) record in the Morgan Hill (April 1984) earthquake.

Note that the San Salvador record has higher peak ground acceleration (PGA) than the Coalinga record ($0.69g$ versus $0.602g$), but it also has a shorter duration, and its "dominant" frequency is much higher than of Coalinga record (Fig. 4). The "dominant" frequencies of the Nicaragua and the Morgan Hill record are very similar, but the former has a lower PGA, $0.325g$. On the other hand, the dominant frequency of the Imperial Valley record is lower than those of both Morgan Hill and Nicaragua, while the duration and peak ground acceleration of this record is comparable to the duration and PGA of the Morgan Hill earthquake. The frequency content of the chosen records is reflected in their acceleration response spectra, shown in Fig. 4.

RESULTS OF DYNAMIC ANALYSES

Natural Frequencies

Table 2 gives the first ten natural frequencies of the CFR dam, calculated with and without the concrete-face slab. The results, as expected, show that the facing slab has only a minor restraining influence on the characteristics of the dam. It is concluded that: (1) There is an increase of the natural frequencies of the dam due to the presence of the slab by only 2–4% (insignificant); and (2) the (transverse) modal shapes of the dam sections with and without slab are practically identical [see Uddin (1992) for details].

Seismic Response

Figs. 5–7 summarize the results of the parametric dynamic response analyses in the form of distribution along the vertical z-axis of the dam of the peak relative elastic displacements, peak shear strains, and peak absolute accelerations (the term elastic is used to distinguish from the sliding block Newmark-type deformations).

It is evident that the top third of the dam (the near crest region) experiences very strong crest

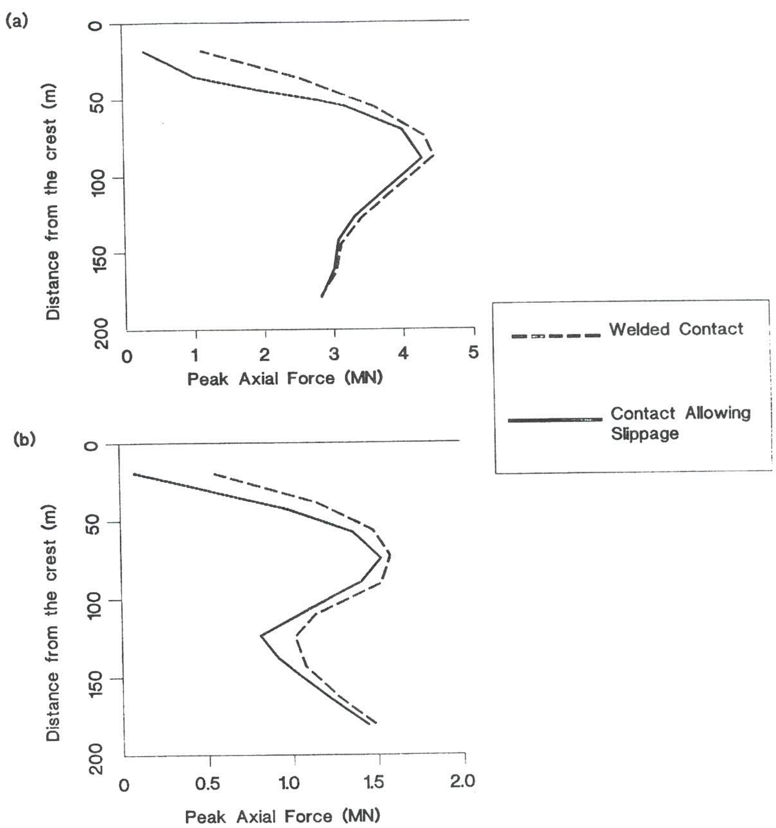

FIG. 11. Effect of Type of Slab-Dam Interface Behavior on Distribution of Peak Axial Force in Slab: (a) 1979 El Centro A1 Excitation; (b) 1973 Nicaragua NU Excitation

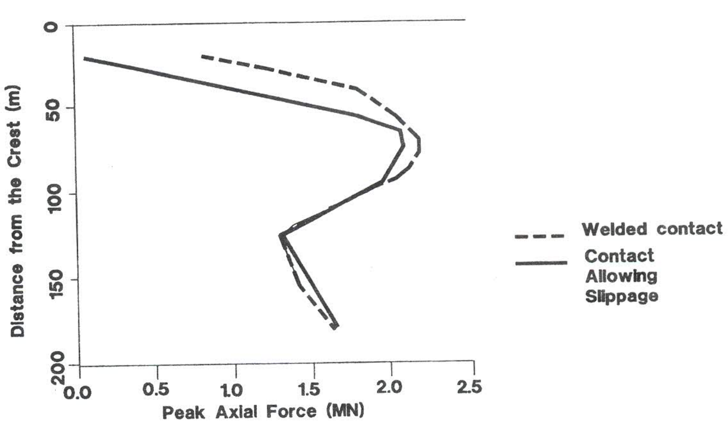

FIG. 12. Effect of Type of Slab-Dam Interface Behavior on Distribution of Peak Axial Force in Slab for 1984 Morgan Hill AD Excitation

accelerations averaging about 1.3g with the very strong excitations and about 0.80g with the moderately strong excitations.

Local shear-strain amplitudes do not exceed the value of 3×10^{-3} (or 0.3%), which is not very large given the intensity of shaking. Peak values of elastic displacement at the crest are about 300 mm for the very strong excitation, but vary from about 50 to 200 mm for the moderately strong excitation records.

Response of Face Slab

Figs. 8–10 depict the face-slab response when Coulomb's friction law governs the behavior of the interface between face slab and dam, and slippage is allowed to occur whenever the seismic contact shear stresses exceed the frictional capacity of that interface.

It is found that the slab experiences very strong axial forces but very small bending moments and shear forces. Figs. 8 and 9 summarize the results of the dynamic response analyses as the distribution along the sloping face of peak axial forces in the slab for the very strong and

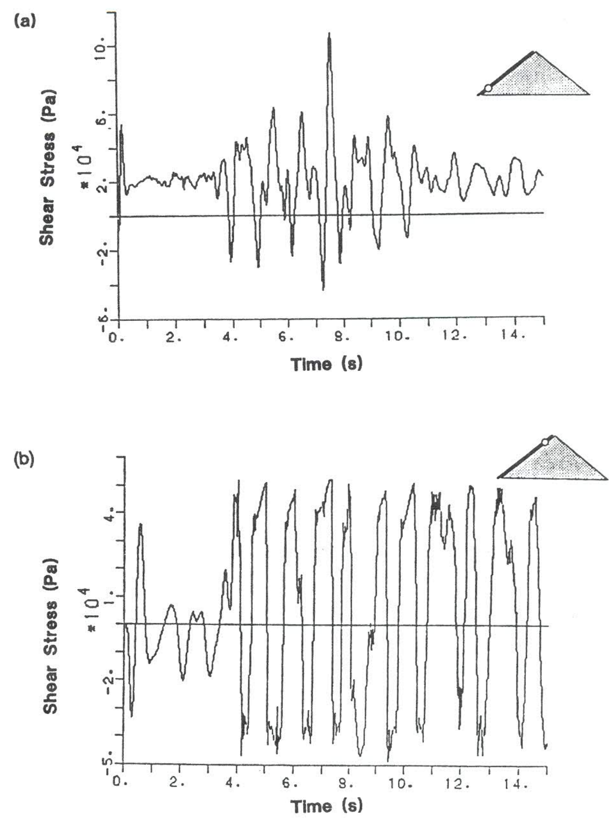

FIG. 13. Shear-Stress History along Slab-Rockfill Interface with Contact Allowing Slippage for 1983 Coalinga PV Excitation: (a) *H*/10 from Base; (b) 9*H*/10 from Base

moderately strong excitation. The implied maximum peak normal stresses are of the order of 12 MPa and 5 MPa, respectively, for the two sets of records, given the 0.40 m thickness of the slab. The former is a very large stress that would undoubtedly produce severe tensile failure in the concrete slab. Therefore, when designing against very strong seismic motions (expected to produce crest acceleration greater than 1g) it is recommended that a thicker and better-reinforced slab be used along with a flatter upstream slope. On the other hand, the value of 5 MPa exceeds only slightly the tensile strength of plain concrete ($\approx$3 to 4 MPa). In the presence of steel reinforcement, such a stress may lead to not more than small-scale cracking of the slab, and may thus be considered barely acceptable in the design.

The distribution of peak contact shear stresses along the slab-rockfill interface is also depicted in Figs. 8 and 9. It is seen that the frictional capacity of this interface is mobilized for the two sets of excitation only in the upper 30 m or 60 m of the slab, where of course the confining water pressure is small and the shaking strong. Below that "sliding" depth, the contact shear stresses remain nearly constant or even decrease with depth, whereas, of course, the frictional capacity increases almost linearly.

Figs. 10–12 compare the peak axial force distribution in the slab obtained under the assumptions of a "welded" interface allowing no slippage between slab and rockfill, and a "sliding" interface. The response of the slab is found to be different in the two cases. The (unrealistic, but used in earlier studies) "welded" contact leads to an increase of about 20% of the maximum peak axial force in the slab.

Fig. 13 shows the typical contact shear-stress history at different locations of the slab for the Coalinga excitation. Due to the presence of large water pressures onto the slab, the lower portion of the slab-rockfill interface experiences stresses that fluctuate about a nonzero static stress [Fig. 13(a)]. On the other hand, at the upper part of the slab (where low confinement causes slippage and separation of the slab from the rockfill) shear stresses fluctuate about a nearly zero static stress [Fig. 13(b)].

CONCLUSIONS

There is presently little analytical and essentially no observational evidence on the behavior of concrete-face slabs during strong seismic shaking. The choice of slab thickness and steel reinforcement is based solely on precedent, with performance under static loads being the only design consideration. To fill this gap, a dynamic FE study of the response of a typical 100-m CFR dam to strong seismic shaking has been presented using a realistic modeling for the embankment material, the slab, and the slab-rockfill interface. Equivalent-linear analyses have been performed with Coulomb's friction law governing the behavior of the face-slab–rockfill interface. The presented results are thus believed to be realistic. The main conclusions follow.

1. The vibration characteristics of the CFR dams can be estimated with conventional methods, ignoring the slab.
2. Crest accelerations reach values 1.5–3.0 times the peak ground acceleration, depending on the frequency content of the motion relative to the dam's natural frequency(ies).
3. Despite the high levels of crest acceleration (up to 1.50*g*) during the very strong excitation, shear strains do not exceed 3×10^{-3}, thanks to their stiff ("unyielding") rockfill structure. The confining pressure of the reservoir water plays a key role in such stiff response.
4. The consequences of the very high accelerations near the midcrest of the dam are likely to be serious—not so much for the overall safety of the dam, as for the face slab and the crest ("parapet") wall.
5. The face slab experiences very strong axial forces, but insignificant bending moment and shear force. For the strongest shaking (PGA $\approx 0.60g$) the face slab experiences tensile stresses substantially exceeding the likely tensile strength of concrete along most of the slab. Severe cracking of the concrete and failure of inadequate construction joints are thus inevitable. Improved design is a necessity.

These conclusions apply to dams in very wide valleys, for which the plane-strain assumption is valid. Dams built in narrow canyons are likely to develop much higher midcrest accelerations for the same base excitation (Mejia and Seed 1983; Gazetas and Dakoulas 1992). In such cases, slab cracking/failure along with other detrimental effects are even more likely and must be faced in a prudent design, even when the peak ground acceleration is as low as 1/3*g*. Particularly vulnerable to such high accelerations are the crest ("parapet") walls, which need significant redesigning or must be omitted altogether.

APPENDIX. REFERENCES

Arrau, L., Ibarra, and Nogurea, G. (1985). "Performance of Cogoti Dam under seismic loading." *Proc. of Symp. on Concrete-Face Rockfill Dams—Design, Construction, and Performance*. ASCE, New York, N.Y., 1–14.

Bathe, K.-J., and Mijailovich, S. (1988). "Finite element analysis of frictional contact problems." *Theoretical and Appl. Mech., Spec. Issue, Supplement No. 1 to (0750-7240/1988)*, Vol. 7, 31–44.

Bureau, G., Volpe, R. L., Roth, W., and Udaka, T. (1985). "Seismic analysis of concrete face rockfill dams." *Proc. of Symp. on Concrete-Face Rockfill Dams—Design, Construction, and Performance*. ASCE, New York, N.Y., 479–508.

Elgamal, A.-W. M., Scott, R. F., Succarieh, M. F., and Yan, L. (1990). "La Villita Dam response during five earthquakes including permanent deformation." *J. Geotech. Engrg.*, ASCE, 116(10), 1443–1462.

Fitzpatrick, M., Cole, B., Kinstler, F., and Knoop, B. (1985). "Design of concrete face rockfill dams." *Proc. of Symp. on Concrete-Face Rockfill Dams—Design, Construction, and Performance*. ASCE, New York, N.Y., 410–434.

Cooke, J. B., and Sherard, J. L. (1985). *Proc. of Symp. on Concrete-Face Rockfill Dams—Design, Construction, and Performance*. ASCE, New York, N.Y.

Gazetas, G. (1981a). "Longitudinal vibrations of embankment dams." *J. Geotech. Engrg.*, ASCE, 107(1), 21–40.

Gazetas, G. (1981b). "Vertical oscillation of earth and rockfill dams: analysis and field observation." *Soils and Found.*, Tokyo, Japan, 21(4), 265–277.

Gazetas, G. (1987a). "Seismic response of earth dams: some recent developments." *Soil Dynamics and Earthquake Engrg.*, 6(1), 1–47.

Gazetas, G. (1987b). "Discussion of seismic analysis of concrete-face rockfill dams." *J. Geotech. Engrg.*, ASCE, 113(10), 1247–1251.

Gazetas, G., and Dakoulas, P. (1992). "Seismic analysis and design of rockfill dams: state of the art." *Soil Dynamics and Earthquake Engrg.*, Vol. 2, 27–61.

Gazetas, G., and Uddin, N. (1994). "Permanent deformation on preexisting sliding surfaces in dams." *J. Geotech. Engrg.*, ASCE, 120(11), 2041–2061.

Guros, F. B., Thiers, G. R., Wathen, T. R., and Buckles, C. E. (1984). "Seismic design of concrete-faced rockfill dams." *Proc., 8th World Conf. on Earthquake Engrg.*, San Francisco, Calif., Vol. III, 317–323.

Han, G., Kong, X., and Li, J. (1988). "Dynamic experiments and numerical simulations of model concrete-face rockfill dams." *Proc., 9th World Conf. on Earthquake Engrg.*, Tokyo-Kyoto, Japan, Vol. 6.

Makdisi, F. I., and Seed, H. B. (1979). "Simplified procedure for evaluating embankment response." *J. Geotech. Engrg.*, ASCE, 105(12), 1427–1434.

Mejia, L. H., Seed, H. B., and Lysmer, J. (1982). "Dynamic analysis of earth dams in three dimensions." *J. Geotech. Engrg.*, ASCE, Vol. 108, 1586–1604.

Mejia, L. H., and Seed, H. B. (1983). "Comparison of 2D and 3D dynamic analysis of earth dams." *J. Geotech. Engrg.*, ASCE, 109(11), 1383–1398.

Seed, H. B., Seed, R. B., Lai, S. S., and Khamenehpour, B. (1985). "Seismic design of concrete-face rockfill dams." *Proc. of Symp. on Concrete-Face Rockfill Dams—Design, Construction, and Performance*, ASCE, New York, N.Y., 459–478.

Seed, H. B., Wong, R. T., Idriss, I. M., and Tokimatsu, K. (1986). "Moduli and damping factors for dynamic analysis of cohesionless soils." *J. Geotech. Engrg.*, ASCE, 112(11), 1016–1032.

Sherard, J. L., and Cooke, J. B. (1987). "Concrete-face rockfill dam: I. Assessment and II. Design." *J. Geotech. Engrg.*, 113(10), 1096–1132.
Uddin, N. (1992). "Seismic analysis of earth-core and concrete-face rockfill dams," PhD thesis, State Univ. of New York at Buffalo, N.Y.
Watabe, M., et al. (1992). "Large scale field tests on quarternary sand and gravel deposits for seismic siting technology." *Proc., 2nd Int. Conf. on Recent Adv. in Geotech. Earthquake Engrg. and Soil Dynamics*, Univ. of Missouri-Rolla, Rolla, Mo., Vol. I, 271–289.